Korean J. Chem. Eng., 39(8), 2211-2216 (2022)
DOI: 10.1007/s11814-021-1044-5

pISSN: 0256-1115
eISSN: 1975-7220

Structure determination of clathrate hydrates formed from alcoholic guests with NH_4F and H_2O

Dong Hyun Kim*,‡, Ki Hun Park*,‡, Minjun Cha*,,†, and Ji-Ho Yoon***,****,†**

*Department of Integrated Energy and Infra System, Kangwon National University, Kangwondaehak-gil, 1, Chuncheon-si, Gangwon-do 24341, Korea
**Department of Energy and Resources Engineering, Kangwon National University, 1 Kangwondaehak-gil, Chuncheon-si, Gangwon-do 24341, Korea
***Department of Energy and Resource Engineering, Korea Maritime and Ocean University, 727 Taejong-ro, Yeongdo-gu, Busan 49112, Korea
****Department of Convergence Study on the Ocean Science and Technology, Ocean Science and Technology (OST) School, Korea Maritime and Ocean University, Busan 49112, Korea
(*Received 17 November 2021 • Revised 9 December 2021 • Accepted 16 December 2021*)

Abstract−The characteristic behavior of alcohol guest inclusions and interactions occurring within binary cyclobutanemethanol (CBM)+methanol (MeOH) and cyclopentanemethanol (CPeM)+MeOH hydrates with hydrate lattices consisting of NH_4F and H_2O was investigated using crystal structure analysis with Rietveld refinement. The crystal structure of our hydrate systems was in the cubic *Fd-3m* space group. CBM or CPeM was captured within the large $5^{12}6^4$ cages of structure II (sII) hydrates, but the effective molecular size of CBM and CPeM was larger than the large cavity size of common sII hydrates. Therefore, the hydroxyl moiety of the CBM and CPeM could interact with the host framework of clathrate hydrates via hydrogen bonding. Similarly, MeOH was encapsulated within the small 5^{12} cages of the sII hydrates, but the Rietveld analysis results indicated that the thermal displacement parameters of the encapsulated MeOH were abnormally high, suggesting off-centered positioning of MeOH and potential host-guest interaction within the small 5^{12} cages of the sII hydrates. These results provide useful insight into the complex nature of host-guest inclusion chemistry.

Keywords: Clathrate Hydrate, Rietveld Analysis, Structure Identification, Alcohol Guest, Hydrogen Bonding

INTRODUCTION

Clathrate hydrates are crystalline inclusion compounds formed by hydrogen-bonded structures as a host cage and guest molecules encapsulated within the host cage [1,2]. Due to the ability of clathrate hydrates to store or separate gaseous molecules within their hydrate cages, they receive considerable attention for energy and environmental applications [3-12]. Conversely, clathrate hydrates are also a problem in oil and gas pipelines because their formation in pipelines may cause blockages [13,14]. Therefore, numerous studies report the prevention of clathrate hydrate formation using chemical additives [13,14].

Alcohols are common thermodynamic inhibitors of clathrate hydrate formation via strong hydrogen bonding with H_2O, but recent findings report the inclusion of certain larger alcohol molecules within the hydrate cages [15-27]. Several larger monohydroxy alcohols, such as propanols (1- and 2-propanol) [15-19], butanols (1-, *iso*-, and *tert*-butanol) [20], pentanols (2-methyl-2-butanol, 3-methyl-2-butanol, 3-methyl-1-butanol, and 2,2-dimethyl-1-propanol) [21,22], and cyclic alcohols (cyclopropanemethanol, -butanemethanol, and -pentanemethanol) [7,23,27], may form cubic structure II (sII) or hexagonal structure H (sH) hydrates in the presence of help gas (CH_4 or Xe). 3-Methyl-1-butanol and 2,2-dimethyl-1-propanol, in particular, are sII hydrate-forming agents in the presence of methane gas, but their molecular size is much larger than the large cavity sizes of common sII hydrates [22]. However, Cha et al. revealed that the host-guest hydrogen bonding occurring in hydrate systems allows 3-methyl-1-butanol and 2,2-dimethyl-1-propanol to fit into the large cages of sII hydrates [22]. These alcohols contain monohydroxy moieties in their molecular structure, but the inclusion behavior of several larger monohydroxy alcohols may be due to the balance between their hydrophobic-hydrophilic parts, suggesting that monohydroxy moieties in their molecular structures are insignificant in hydrate formation. Unlike several larger monohydroxy alcohols, direct evidence of methanol (MeOH) enclathration within hydrate cages was not reported until 2013 [28-32], and Shin et al. [33] reported MeOH occupation of the small cages of sII hydrates using the quenching method for a solution of tetrahydrofuran-H_2O-MeOH at 183 K. However, the cage occupancy of MeOH was only 4.4% at equilibrium [33]. Therefore, the management of host-guest hydrogen bonding may be critical in stabilizing the hydrate structure with alcohol guest molecules, and they suggested the doping of NH_4F into the host H_2O to demon-

†To whom correspondence should be addressed.
E-mail: minjun.cha@kangwon.ac.kr, jhyoon@kmou.ac.kr
‡These authors are equally contributed.

strate the role of MeOH as a help guest [34,35].

Herein, we demonstrate the enclathration of MeOH and several larger monohydroxy alcohols (cyclobutanemethanol (CBM) and -pentanemethanol (CPeM)) within the small and large cages of sII hydrates with hydrate lattices consisting of H_2O and NH_4F. The characteristic behavior of the alcohol guest molecules within the NH_4F-doped hydrate cages was investigated via structural identification of the binary (CBM+MeOH) or (CPeM+MeOH) hydrates with H_2O and NH_4F using powder X-ray diffraction (PXRD) with Rietveld refinement.

EXPERIMENTAL DETAILS

Distilled H_2O (Samchun Pure Chemical, Pyeongtaek-si, South Korea), CBM ($C_4H_7CH_2OH$, 98.0 mol% purity, Tokyo Chemical Industry, Tokyo, Japan), CPeM ($C_5H_9CH_2OH$, 98.0 mol% purity, Tokyo Chemical Industry), NH_4F (98 mol% purity, Sigma-Aldrich, St. Louis, MO, USA), and MeOH (CH_3OH, 98 mol% purity, Sigma-Aldrich) were used for synthesizing the binary (CBM+MeOH) and (CPeM+MeOH) hydrates with hydrate lattices consisting of NH_4F and H_2O (H_2O/NH_4F).

To prepare the binary (CBM+MeOH) and (CPeM+MeOH) hydrates (H_2O/NH_4F), the following procedure was used: NH_4F was dissolved in distilled H_2O. A homogeneous 25 mol% NH_4F solution was quenched dropwise at a liquid nitrogen temperature. The frozen NH_4F solutions were crushed to fine powder (~100 μm particles) using liquid nitrogen and immersed in pre-cooled (~193 K) mixed alcohol solutions. The unit cell structure of the sII hydrate consists of 8 large and 16 small cages. Therefore, two mixed alcohol solutions were prepared: 1) liquid CBM (33.3 mol%)+MeOH (66.7 mol%) and 2) liquid CPeM (33.3 mol%)+MeOH (66.7 mol%). The mixed alcohol solutions containing the frozen NH_4F samples were placed in a freezer (~193 K) for a week. In mixed alcohol solutions, the crushed samples (the frozen NH_4F solutions) were transformed to (CBM+MeOH) or (CPeM+MeOH) hydrate (H_2O/NH_4F) at 193 K. The hydrate conversion process from the frozen NH_4F solutions to (CBM+MeOH) or (CPeM+MeOH) hydrate (H_2O/NH_4F) at 193 K could be a slow process, and thus the vials containing the mixed alcohol solutions with the frozen NH_4F samples were shaken time to time to promote the conversion of hydrate samples. After hydrate formation, unreacted CBM/MeOH and CPeM/MeOH were removed under vacuum for 3 h in a freezer [34,35]. The powdered samples were then ground using a 100 μm sieve and subjected to PXRD.

PXRD of the (CBM+MeOH) or (CPeM+MeOH) hydrate (H_2O/NH_4F) samples was performed at 100 K using the 2D Supramolecular Crystallography beamline (with a synchrotron radiation of 0.900 Å) at the Pohang Accelerator Laboratory (PAL). A polyimide tube (0.635 mm I.D.; Antylia Scientific, Vernon Hills, IL, USA) was filled with the ground hydrate sample and attached to a magnetic goniometer. For data collection and processing (2D diffraction images to 1D diffraction patterns), PAL BL2D-SMDC and FIT2D (European Synchrotron Radiation Facility, Grenoble, France) software were employed [36,37]. The obtained PXRD patterns of the (CBM+MeOH) and (CPeM+MeOH) hydrate (H_2O/NH_4F) samples were refined using the FULLPROF program for the Rietveld analyses [38,39].

RESULTS AND DISCUSSION

The characteristic behavior of alcohol guest inclusions and interactions occurring within the (CBM+MeOH) and (CPeM+MeOH) hydrates (H_2O/NH_4F) was investigated by Rietveld analysis using the FULLPROF software [38,39]. The atomic scattering factors of hydrogen atoms are very small, but the effects of hydrogen atoms on the diffraction pattern may be considerable. Therefore, $-CH_3$, $-CH_2-$, -CH-, -OH, and H_2O virtual atomic species were used in this study by adding atomic scattering factors [7,18,23,27]. Due to their very similar scattering factors, the host framework components of H_2O and NH_4F were indistinguishable [34,35]. During structure refinement, zero shift, scale, peak shape, and thermal displacement parameters, atomic coordinates, lattice parameters, and site occupancies were refined. The structural models of the CBM and CPeM molecules within the large $5^{12}6^4$ cages of the sII hydrate were adopted using previously reported models (Fig. 1) [7,27]. Alcohol guest molecules as rigid bodies are positioned at the centers of the large $5^{12}6^4$ (for CBM and CPeM molecules) and small 5^{12} (for the MeOH molecule) cages within the sII hydrates. Although MeOH enclathration within the large $5^{12}6^4$ cages of the sII hydrates is possible, we assumed that the large $5^{12}6^4$ cages are occupied only by the CBM or CPeM.

The refined supramolecular crystallography patterns of the binary

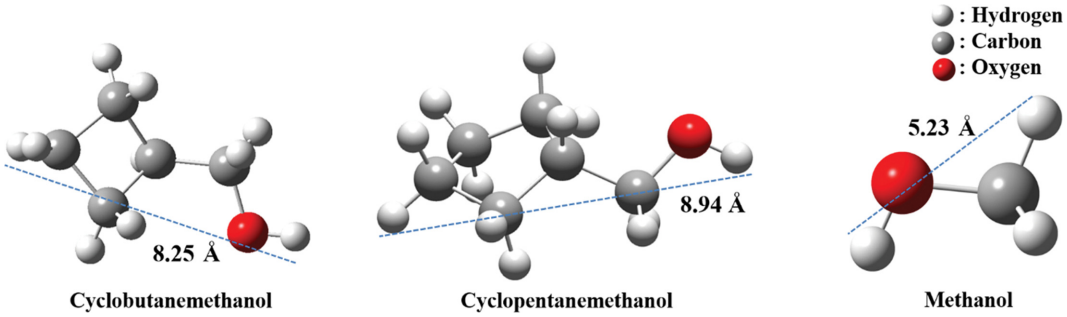

Fig. 1. Calculated conformation and the molecular size of cyclobutanemethanol, cyclopentanemethanol, and methanol (Grey, carbon; white, hydrogen; red, oxygen). Detailed procedures for calculating the atomic sizes of cyclobutanemethanol, cyclopentanemethanol, and methanol can be found in the previous studies [7,18,20,22,23,27].

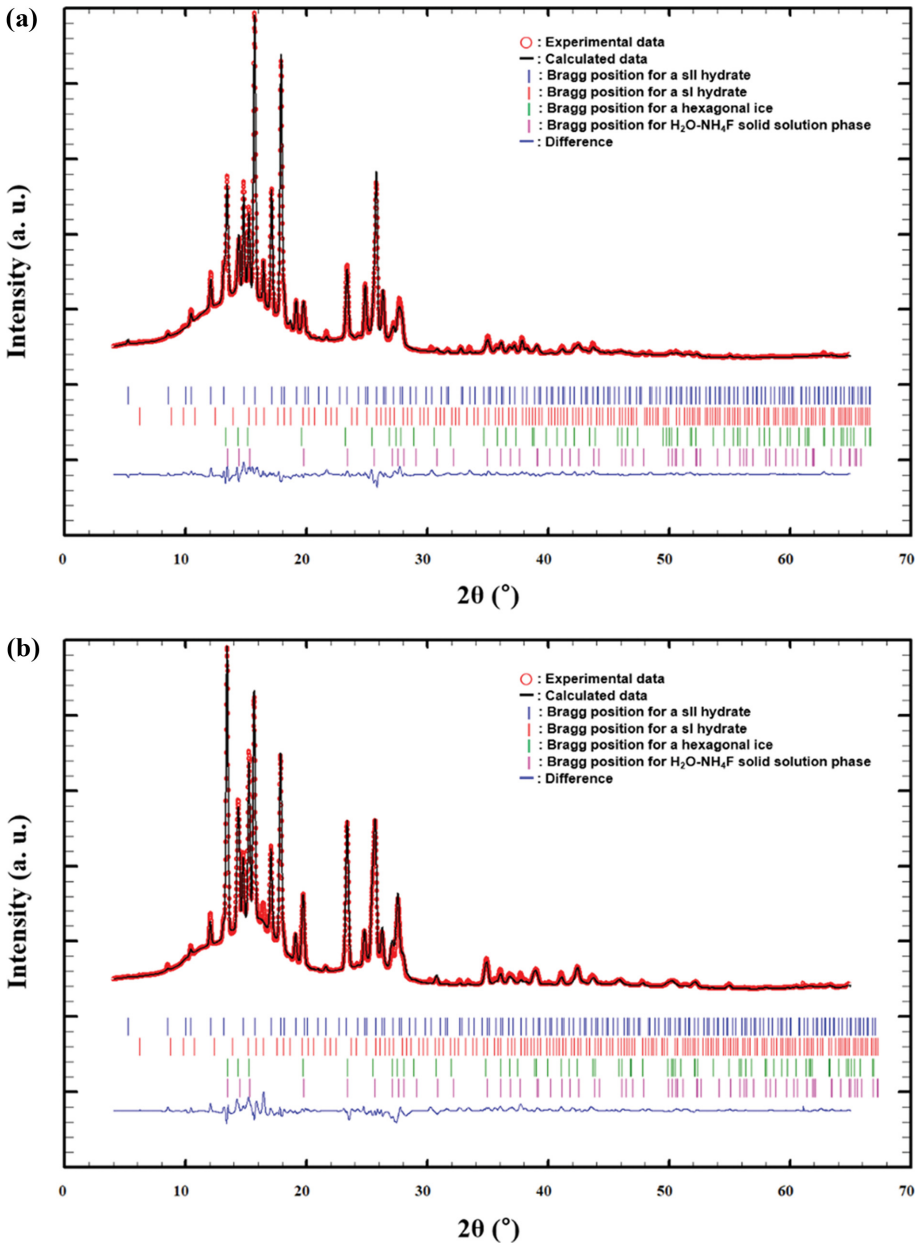

Fig. 2. Supramolecular crystallography pattern of (a) (cyclobutanemethanol+methanol) hydrate (H_2O/NH_4F) measured at 100 K and the Rietveld refinement results (background corrected R_{wp}=10.4% and χ^2=4.94), and (b) (cyclopentanemethanol+methanol) hydrate (H_2O/NH_4F) measured at 100 K and the Rietveld refinement results (background corrected R_{wp}=12.7% and χ^2=8.65). Tick marks indicate the Bragg position for sII hydrate, sI hydrate, the hexagonal ice, and the H_2O/NH_4F solid solution phases, respectively.

(CBM+MeOH) and (CPeM+MeOH) hydrates (H_2O/NH_4F) are shown in Fig. 2. The patterns are well-refined, with reliability factors of background corrected R_{wp}=10.4% and χ^2=4.94 for the (CBM+MeOH) hydrate (H_2O/NH_4F), and background corrected R_{wp}=12.7% and χ^2=8.65 for the (CPeM+MeOH) hydrate (H_2O/NH_4F). The structural parameters (atomic coordinates, thermal displacement parameters, and site occupancies) of the binary (CBM+MeOH) and (CPeM+MeOH) hydrates (H_2O/NH_4F) are listed in Tables 1 and 2. The binary (CBM+MeOH) and (CPeM+MeOH) hydrates (H_2O/NH_4F) are in the cubic *Fd-3m* space group with lattice parameters of 17.10570 (72) and 17.14797 (65) Å, respectively. The hexagonal $P6_3/mmc$ structure of the hexagonal ice, the hexagonal $P6_3/mmc$ structure of the NH_4F solid solution, and the cubic *Pm-3n* structure of the structure I hydrate of the MeOH hydrate (H_2O/NH_4F) are also observed in the refined PXRD pattern. The unit cell systems of the binary (CBM+MeOH) and (CPeM+MeOH) hydrates (H_2O/NH_4F) are 6.937 CBM·12.411 MeOH·136 H_2O/NH_4F and 6.329 CPeM·15.146 MeOH·136 H_2O/NH_4F, respectively. The calculated weight fraction of the binary (CBM+MeOH) hydrate (H_2O/NH_4F) hydrate was 70.2%, with the impurity hexagonal ice (*Ih*), NH_4F solid solution, and structure I hydrate accounting for the remaining 6.2%, 12.1%, and 11.5%, respectively. Similarly, the cal-

Table 1. Atomic coordinates, isotropic temperature factors, and site occupancies for (cyclobutanemethanol+methanol) hydrate (H_2O/NH_4F) (Wa, virtual atomic species for the host framework; SG, virtual atomic species for methanol; LG, virtual atomic species for cyclobutanemethanol)

Atom	x	y	z	B(Å^2)	Site occupancy
Wa^1	0.12500	0.12500	0.12500	4.241	8
Wa^2	0.21777(9)	0.21777(9)	0.21777(9)	4.428	32
Wa^3	0.18318(4)	0.18318(4)	0.37394(9)	7.090	96
SG^1 (CH_3 in MeOH)	−0.01526	0.04148	0.00081	9.166	12.411
SG^2 (OH in MeOH)	0.01349	−0.03667	−0.00071	9.166	12.411
LG^1 (CH_2 in CBM)	0.28826	0.45042	0.41412	0.843	6.937
LG^2 (CH_2 in CBM)	0.37605	0.42991	0.42420	0.843	6.937
LG^3 (CH in CBM)	0.36038	0.35073	0.38219	0.843	6.937
LG^4 (CH_2 in CBM)	0.28321	0.38662	0.34983	0.843	6.937
LG^5 (CH_2 in CBM)	0.42125	0.32235	0.32438	0.843	6.937
LG^6 (OH in CBM)	0.49547	0.32095	0.36305	0.843	6.937

Table 2. Atomic coordinates, isotropic temperature factors, and site occupancies for (cyclopentanemethanol+methanol) hydrate (H_2O/NH_4F) (Wa, virtual atomic species for the host framework; SG, virtual atomic species for methanol; LG, virtual atomic species for cyclopentanemethanol)

Atom	x	y	z	B(Å^2)	Site occupancy
Wa^1	0.12500	0.12500	0.12500	12.215	8
Wa^2	0.21726	0.21726	0.21726	10.264	32
Wa^3	0.18286	0.18286	0.37484	12.144	96
SG^1 (CH_3 in MeOH)	−0.01418	0.03965	0.01312	30.522	15.146
SG^2 (OH in MeOH)	0.01254	−0.03505	−0.01159	30.522	15.146
LG^1 (CH in CPeM)	0.35744	0.38488	0.35586	4.225	6.329
LG^2 (CH_2 in CPeM)	0.38594	0.30543	0.32379	4.225	6.329
LG^3 (CH_2 in CPeM)	0.47517	0.31261	0.32272	4.225	6.329
LG^4 (CH_2 in CPeM)	0.49277	0.35621	0.39910	4.225	6.329
LG^5 (CH_2 in CPeM)	0.42611	0.41650	0.40673	4.225	6.329
LG^6 (CH_2 in CPeM)	0.27965	0.38071	0.39865	4.225	6.329
LG^7 (OH in CPeM)	0.25102	0.45818	0.41106	4.225	6.329

culated weight fraction of the binary (CPeM+MeOH) hydrate (H_2O/NH_4F) hydrate was 69.0%, with the impurity hexagonal ice (*Ih*), NH_4F solid solution, and structure I hydrate accounting for the remaining 1.5%, 15.7%, and 13.8%, respectively. Even though we tried to remove the unreacted CBM/MeOH and CPeM/MeOH, there was unreacted CBM/MeOH and CPeM/MeOH as well as powdered NH_4F solid solution due to the low vapor pressure of alcohol molecules at 193 K. The residual MeOH and powdered NH_4F solid solution may form structure I hydrate [34,35]. In addition, hydrate samples can occasionally be exposed to the air during experiments, and thus there can be the impurity of ice in our hydrate samples. In our previous studies, the crystal structure of the binary ($CBM+CH_4$) and ($CPeM+CH_4$) hydrates (H_2O) with hydrate lattices consisting of H_2O was cubic *Fd-3m* hydrates with lattice parameters of 17.23630 and 17.28227 Å, respectively [7,27]. Shin et al. reported that the lattice parameters of NH_4F-doped clathrate hydrates decrease as the NH_4F concentration in the solid NH_4F solution increases [34,35]. Therefore, the decrease in the cubic lattice parameters of the binary (CBM+MeOH) and (CPeM+MeOH) hydrates (H_2O/NH_4F) compared to those of the binary ($CBM+CH_4$) and ($CPeM+CH_4$) hydrates (H_2O) may be due to the slightly different hydrogen bond lengths (2.71 and 2.76 Å for NH···F and OH···O, respectively) [34,35]. In addition, the cage occupancy of guest molecules in the binary (CBM+MeOH) and (CPeM+MeOH) hydrates (H_2O/NH_4F) compared to that of the binary ($CBM+CH_4$) and ($CPeM+CH_4$) hydrates (H_2O) slightly decreased, but the differences in the cage occupancy for both hydrate systems are not significant [7,27].

CBM, CPeM, and MeOH molecules with full symmetries within the large $5^{12}6^4$ (for CBM and CPeM molecules) and small 5^{12} (for MeOH molecules) cages of the sII hydrates are shown in Fig. 3. The CBM and CPeM molecules within the large $5^{12}6^4$ cages of the sII hydrates are randomly distributed. The shortest distances between host and guest oxygen atoms in the CBM and CPeM structures are 2.37 and 2.29 Å, respectively (Fig. 4). Therefore, hydrogen bonding may occur between the hydroxyl functional groups of the CBM or CPeM molecules and the host framework (H_2O/NH_4F) [7,18,23,27]. In addition, host-guest hydrogen interactions in the large $5^{12}6^4$ cages of the binary (CBM+MeOH) and (CPeM+MeOH) hydrates (H_2O/NH_4F) are predominantly observed at the

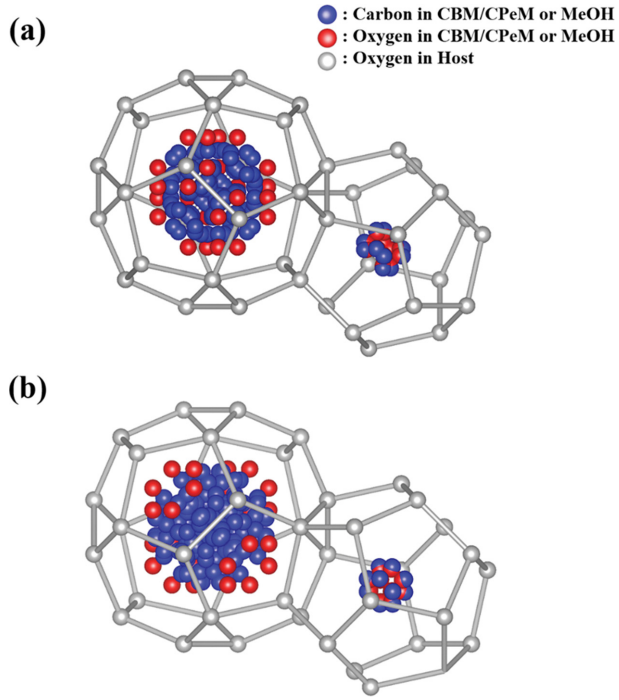

Fig. 3. Crystal structure and guest positions of (a) (cyclobutanemethanol+methanol) hydrate (H_2O/NH_4F) and (b) (cyclopentanemethanol+methanol) hydrate (H_2O/NH_4F) obtained by Rietveld analysis. Distribution of guest molecules in small and large cages of (cyclobutanemethanol+methanol) and (cyclopentanemethanol+methanol) hydrates (H_2O/NH_4F) with full symmetry (grey; oxygen in water host molecule; red, oxygen in hydroxyl group of guest molecule; blue, carbon in guest molecule).

hexagonal faces owing to the relatively weak hydrogen bonding of the host framework at these positions in the sII hydrate. We cannot completely discount the possibility of an off-centered guest positional disorder from the center of the large $5^{12}6^4$ cage, but the thermal displacement parameters of the CBM and CPeM molecules compared to those of the host framework (H_2O/NH_4F) are relatively small. Therefore, a significant degree of guest positional disorder within the large $5^{12}6^4$ cages is unlikely.

Similar to the CBM and CPeM molecules within the large $5^{12}6^4$ cages, the MeOH molecules within the small 5^{12} cages of the sII hydrate are also isotropically distributed (Fig. 3). The patterns are well-refined using Rietveld refinement. However, the thermal displacement parameters of MeOH at the centers of the small 5^{12} cages within the sII hydrate are anomalously high, as listed in Tables 1 and 2. Therefore, a significant degree of guest positional disorder within the small 5^{12} cages may occur, suggesting possible host-guest hydrogen interaction within the small 5^{12} cages or the incorporation of the MeOH hydroxyl group into the host framework (H_2O/NH_4F). Using Rietveld refinement, the H_2O/NH_4F host frameworks of the binary (CBM+MeOH) and (CPeM+MeOH) hydrates (H_2O/NH_4F) were indistinguishable; thus, the distances between the host atoms (Fig. 4) could be affected by this indistinguishable property [34,35,40].

These findings, regarding the guest inclusions and interactions occurring within the binary (CBM+MeOH) and (CPeM+MeOH) hydrates (H_2O/NH_4F), provide fundamental data regarding the unique nature of host-guest inclusion compounds and insight with respect to the crystal engineering of clathrate hydrates.

CONCLUSIONS

We prepared binary (CBM+MeOH) and (CPeM+MeOH) hydrates with hydrate lattices consisting of NH_4F and H_2O and identified the characteristic behavior of the alcohol guest inclusions and interactions occurring within the hydrate systems. The Rietveld analyses of the binary (CBM+MeOH) and (CPeM+MeOH) hydrates (H_2O/NH_4F) revealed that the crystal structure of our hydrate systems was cubic *Fd-3m* and the hydroxyl group of CBM or CPeM may interact with the host framework via hydrogen bonding. In addition, anomalously high thermal displacement parameters of the MeOH at the centers of the small 5^{12} cages within the sII hydrates indicate significant degree of guest positional disorder within the small 5^{12} cages. These results provide useful insight into the complex nature of host-guest inclusion chemistry.

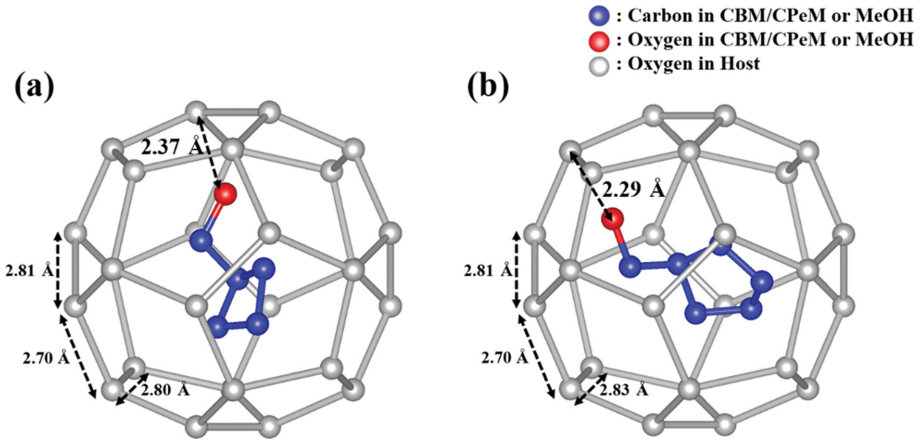

Fig. 4. The (a) cyclobutanemethanol and (b) cyclopentanemethanol in the large ($5^{12}6^4$) cage (H_2O/NH_4F) of sII hydrate (grey; oxygen in water host molecule; red, oxygen in hydroxyl group of guest molecule; blue, carbon in guest molecule).

ACKNOWLEDGEMENT

This study was supported by the National Research Foundation of Korea (NRF) grants (NRF-2019R1F1A1058167 and NRF-2021 R1F1A1049420) funded by the Korea government (MSIT; Ministry of Science and ICT). High resolution powder diffraction (HRPD) patterns are collected from the beamline (2D) at Pohang Accelerator Laboratory.

REFERENCES

1. E. D. Sloan, *Nature*, **426**, 353 (2003).
2. E. D. Sloan and C. A. Koh, *Clathrate hydrates of natural gases*, 3rd ed., CRC Press, Boca Raton (2008).
3. H. Mimachi, S. Takeya, A. Yoneyama, K. Hyodo, T. Takeda, Y. Gotoh and T. Murayama, *Chem. Eng. Sci.*, **118**, 208 (2014).
4. S. Machida, H. Hirai, T. Kawamura, Y. Yamamoto and T. Yagi, *J. Phys. Chem. Solids*, **71**, 1324 (2010).
5. H. Ogawa, N. Imura, T. Miyoshi, R. Ohmura and Y. H. Mori, *Energy Fuels*, **23**, 849 (2009).
6. J. H. Yoon, J. Han, J. Park, S. Choi, S. H. Yeon and H. Lee, *J. Phys. Chem. Solids*, **69**, 1432 (2008).
7. K. H. Park, D. H. Kim and M. Cha, *Chem. Eng. J.*, **421**, 127835 (2020).
8. G. Ko, J. Lee and Y. Seo, *Chem. Eng. J.*, **405**, 126956 (2021).
9. T. Ikeda, O. Yamamuro, T. Matsuo, K. Mori, S. Torii, T. Kamiyama, F. Izumi, S. Ikeda and S. Mae, *J. Phys. Chem. Solids*, **60**, 1527 (1999).
10. I. Cha, S. Lee, J. D. Lee, G. W. Lee and Y. Seo, *Environ. Sci. Technol.*, **44**, 6117 (2010).
11. V. R. Belosludov, Y. Y. Bozhko, K. V. Gets, O. S. Subbotin and Y. Kawazoe, *J. Phys. Conf. Ser.*, **1128**, 012086 (2018).
12. A. Falenty, W. F. Kuhs, M. Glockzin and G. Rehder, *Energy Fuels*, **28**, 6275 (2014).
13. K. H. Park, D. Jeong, J. H. Yoon and M. Cha, *Fluid Phase Equilib.*, **493**, 43 (2019).
14. M. Cha, K. Shin, J. Kim, D. Chang, Y. Seo, H. Lee and S. P. Kang, *Chem. Eng. Sci.*, **99**, 184 (2013).
15. M. Cha, K. Shin and H. Lee, *Korean J. Chem. Eng.*, **34**, 2514 (2017).
16. J.-J. Max, S. Daneault and C. Chapados, *Can. J. Chem.*, **80**, 113 (2002).
17. S. Alavi, S. Takeya, R. Ohmura, T. K. Woo and J. A. Ripmeester, *J. Chem. Phys.*, **133**, 074505 (2010).
18. K. H. Park and M. Cha, *Korean J. Chem. Eng.*, **37**, 151 (2020).
19. R. Ohmura, S. Takeya, T. Uchida and T. Ebinuma, *Ind. Eng. Chem. Res.*, **43**, 4964 (2004).
20. Y. Youn, M. Cha and H. Lee, *ChemPhysChem*, **16**, 2876 (2015).
21. S. Hong, S. Moon, Y. Lee, S. Lee and Y. Park, *Chem. Eng. J.*, **363**, 99 (2019).
22. M. Cha, K. Shin and H. Lee, *J. Phys. Chem. B*, **113**, 10562 (2009).
23. K. H. Park, K. Shin and M. Cha, *J. Phys. Chem. C*, **123**, 26777 (2019).
24. E. Kim, Y. K. Jin and Y. Seo, *Fluid Phase Equilib.*, **393**, 85 (2015).
25. Y. H. Ahn, Y. Youn, M. Chaf and H. Lee, *RSC Adv.*, **7**, 12359 (2017).
26. B. Sung, K. Shin, M. Cha, S. Choi, J. Lee, Y. Seo and H. Lee, *J. Chem. Eng. Data*, **55**, 5906 (2010).
27. K. H. Park, D. H. Kim and M. Cha, *Chem. Phys. Lett.*, **779**, 138869 (2021).
28. D. Blake, L. Allamandola, S. Sandford, D. Hudgins and F. Freund, *Sciences*, **254**, 548 (1991).
29. K. D. Williams and J. P. Devlin, *J. Mol. Struct.*, **416**, 277 (1997).
30. K. Koga, H. Tanaka and K. Nakanishi, *J. Chem. Phys.*, **101**, 3127 (1994).
31. G. Notesco and A. Bar-Nun, *Icarus*, **148**, 456 (2000).
32. A. Wallqvist, *J. Chem. Phys.*, **96**, 5377 (1992).
33. K. Shin, K. A. Udachin, I. L. Moudrakovski, D. M. Leek, S. Alavi, C. I. Ratcliffe and J. A. Ripmeester, *Proc. Natl. Acad. Sci. USA*, **110**, 8437 (2013).
34. K. Shin, I. L. Moudrakovski, M. D. Davari, S. Alavi, C. I. Ratcliffe and J. A. Ripmeester, *Cryst. Eng. Comm.*, **16**, 7209 (2014).
35. K. Shin, I. L. Moudrakovski, C. I. Ratcliffe and J. A. Ripmeester, *Angew. Chem. Int. Ed.*, **56**, 6171 (2017).
36. A. P. Hammersley, S. O. Svensson, M. Hanfland, A. N. Fitch and D. Hausermann, *High Pressure Research*, **14**, 235 (1996).
37. J. W. Shin, K. Eom and D. Moon, *J. Synchrotron Radiat.*, **23**, 369 (2016).
38. J. Rodriguez-Carvajal, *Physica B*, **192**, 55 (1993).
39. S. Takeya, K. A. Udachin, I. L. Moudrakovski, R. Susilo and J. A. Ripmeester, *J. Am. Chem. Soc.*, **132**, 524 (2010).
40. S. Takeya, H. Fujihisa, H. Yamawaki, Y. Gotoh, R. Ohmura, S. Alavi and J. A. Ripmeester, *Angew. Chem. Int. Ed.*, **55**, 9287 (2016).